*Geochimica et Cosmochimica Acta* Vol. 52, pp. 2451–2456

0016-7037/88/$3.00 + .00

# Synthetic fluid inclusions: VIII. Vapor-saturated halite solubility in part of the system NaCl-$CaCl_2$-$H_2O$, with application to fluid inclusions from oceanic hydrothermal systems

D. A. VANKO[1], R. J. BODNAR[2] and S. M. STERNER[2]

[1]Department of Geology, Georgia State University, Atlanta, GA 30303, U.S.A.
[2]Department of Geological Sciences, Virginia Polytechnic Institute & State University, Blacksburg, VA 24061, U.S.A.

(*Received February* 16, 1988; *accepted in revised form July* 25, 1988)

**Abstract**—Halite solubility along part of the vapor-saturated liquidus in the system NaCl-$CaCl_2$-$H_2O$ has been determined using the synthetic fluid inclusion technique. Data allow the construction of liquidus isotherms for temperatures up to 500°C and bulk compositions containing >60 wt% total salt and as much as 25 wt% $CaCl_2$. Combined with previous data for the binary system NaCl-$H_2O$ and for the ternary system NaCl-$CaCl_2$-$H_2O$ in the low-salinity, low-temperature region, a preliminary ternary phase diagram can be constructed that remains incomplete only in the $CaCl_2$-rich region.

Results are applied to the interpretation of saline fluid inclusions from quartz veins in oceanic metagabbros, and can be applied to many other natural inclusions containing aqueous solutions with NaCl and $CaCl_2$ the dominant solutes. Microthermometric measurements at equilibrium of the melting temperature of ice [*Tm* (ice)] and of the dissolution temperature of halite [*Tm* (halite)] are sufficient to determine the bulk composition of the NaCl-$CaCl_2$-$H_2O$ fluid.

## INTRODUCTION

EQUILIBRIUM PHASE RELATIONS in the ternary system NaCl-$CaCl_2$-$H_2O$ are known quantitatively only in the low-temperature, water-rich portion of the system (YANATIEVA, 1946). As with the binary system NaCl-$H_2O$, high-temperature, saline compositions are difficult to study because of the tendency for salt precipitation to undermine the sampling process (SOURIRAJAN and KENNEDY, 1962). To avoid direct sampling investigators have utilized indirect techniques such as monitoring pressure as a function of temperature to identify breaks in slope which are indicative of a phase change (POTTER *et al.*, 1977), and differential thermal analysis (GUNTER *et al.*, 1983; CHOU, 1987). With these techniques, the temperature at which a known vapor-saturated solution reaches halite saturation can be inferred.

Recently, synthetic fluid inclusions have been utilized to study saline compositions in the systems NaCl-$H_2O$ (STERNER and BODNAR, 1984; BODNAR *et al.*, 1985) and NaCl-KCl-$H_2O$ (STERNER *et al.*, 1988). The technique involves trapping single-phase fluids of known composition in natural quartz at elevated pressure and temperature. At room temperature, however, the saline inclusions contain vapor, liquid, and a daughter crystal of halite. By reheating the inclusions in a standard heating/freezing stage, the temperature of halite dissolution [*Tm* (halite)] is determined; this temperature represents the vapor-saturated halite solubility as long as the inclusion undergoes near-simultaneous disappearance of both halite and vapor (CHOU, 1987; STERNER *et al.*, 1988). Using the synthetic fluid inclusion technique, we have extended data in the NaCl-$CaCl_2$-$H_2O$ ternary to include the NaCl-rich portion of the halite liquidus (to 25 wt% $CaCl_2$ maximum) up to temperatures of 500°C and total salinities > 60 wt%.

A revised phase diagram for the vapor-saturated ternary system NaCl-$CaCl_2$-$H_2O$ allows modelling of natural fluid inclusions that contain halite daughter crystals and NaCl-$CaCl_2$ brines. Such fluid inclusions occur in mid-ocean ridge systems (VANKO, 1988), skarns (*e.g.*, KWAK and TAN, 1981), uranium deposits (*e.g.*, PAGEL *et al.*, 1980; FUZIKAWA, 1982), gold deposits (*e.g.*, ROBERT and KELLY, 1987), Mississippi Valley-type ores (*e.g.*, TAYLOR *et al.*, 1983; ROEDDER, 1984), and the Salton Sea geothermal system (MCKIBBEN *et al.*, 1988).

## METHODS

The synthetic fluid inclusion technique is fully described in BODNAR and STERNER (1987) and is only briefly summarized here. Experiments were conducted in Pt capsules to minimize contamination resulting from the corrosive effects of chloride brines at elevated temperatures. Three $CaCl_2$-$H_2O$ solutions were prepared from reagent grade $CaCl_2 \cdot 4H_2O$. A small weighed portion of one of the $CaCl_2$-$H_2O$ fluids was added to each experimental capsule together with enough reagent grade NaCl to give a desired bulk fluid composition. A fractured natural quartz core approximately 4.5 mm in diameter and 10 mm long was inserted into the capsule, and the capsule sealed. The loaded capsules were weighed and heated overnight at >100°C to check for leaks. Surviving capsules were loaded into cold-seal hydrothermal bombs and run for 7 days at 700°C and 2.0 to 4.5 kbar (Table 1). The actual *P-T* conditions were chosen for each composition in light of previous data for the system NaCl-$H_2O$. The aim was to synthesize fluid inclusions that, on heating, would undergo nearly simultaneous halite dissolution and vapor disappearance.

After quenching, the healed quartz cores were removed and sliced into 5–6 discs, each about 1 mm thick. These were polished for heating and freezing determinations, which were done on separate discs to avoid any complications from possible stretching or decrepitation.

Microthermometric measurements were made with a Fluid Inc.-adapted USGS-type heating/freezing stage mounted on a Zeiss petrographic microscope. Temperatures of phase changes were measured with a chromel-constantan thermocouple directly on the sample chip. Measurements were calibrated using synthetic fluid inclusions having known phase transitions at −56.6°C, 0.0°C, and +374°C. Occasional use was made of ice baths and of triply distilled Hg (*Tm* = −38.89°C). During calibrations, the temperatures indicated by the thermocouple were always within 0.2°C of the −56.6°C standard, within 0.1°C of the 0.0°C standard, and within 1.0°C of the 374°C standard. Therefore, the accuracy of measurements on unknowns is thought to be ±0.2°C during freezing runs and ±1.0°C during heating runs.

## RESULTS OF SYNTHETIC INCLUSION MICROTHERMOMETRY

Liquidus relationships in the low salinity portion of the ternary system NaCl-$CaCl_2$-$H_2O$ are summarized in CRAW-

Table 1. Results of heating measurements on synthetic inclusions

| Sample | Composition[1] | P(kb) | Tm(halite) | Avg. Tm(halite)[2] |
|---|---|---|---|---|
| 1 | 28.1/7.2/64.7 | 4.5 | 219.6-221.4 | 220.6 (12) |
| 2 | 39.6/6.0/54.4 | 3.5 | 356.5-358.4 | 357.3 (15) |
| 3 | 49.8/5.0/45.2 | 2.0 | 440.6-443.5 | 442.5 (7) [3] |
| | | | 439.6-448.2 | 441.9 (10)[4] |
| 4 | 60.1/4.0/35.9 | 2.0 | 507.0-512.2 | 510.0 (17) |
| 5 | 19.4/16.1/64.5 | 4.5 | 188.3-199.7 | 191.8 (12) |
| 6 | 29.7/14.1/56.2 | 3.5 | 294.4-295.9 | 295.0 (13) |
| 8 | 49.8/10.0/40.2 | 2.0 | 456.9-458.8 | 458.1 (14) |
| 9 | 15.2/25.4/59.3 | 3.5 | 205-206 | 205.6 (10) |
| 11 | 35.0/19.5/45.5 | 2.25 | 372.0-374.6 | 373.3 (13) |
| 12 | 45.7/16.3/38.0 | 2.0 | 448.0-449.7 | 448.9 (12) |

[1] Wt % $NaCl/CaCl_2/H_2O$.
[2] Temperatures in degrees C; number of inclusions measured in parentheses.
[3] Measured Tm(halite) for seven inclusions having Tm(halite) less than the homogenization temperature.
[4] Measured Tm(halite) for ten inclusions having Tm(halite) equal to the homogenization temperature; see text for discussion.

FORD (1981) and SHEPHERD *et al.* (1985), and are shown in Fig. 1. Phase boundaries and isotherms are based on the data of YANATIEVA (1946) and LINKE (1958). The ice-hydrohalite eutectic and the freezing point depressions along the NaCl-$H_2O$ binary between ice and hydrohalite are from HALL *et al.* (1988). The system has a ternary eutectic at about −52°C (Te; Fig. 1). The reaction curve separating the halite and hydrohalite ($NaCl \cdot 2H_2O$) liquidus fields closely parallels the hydrohalite-ice cotectic (Fig. 1). Ice, hydrohalite, and antarcticite ($CaCl_2 \cdot 6H_2O$) form the three solid phases at the eutectic. Bulk compositions of the fluid inclusions prepared for this study are plotted in Fig. 1. These were chosen so that the resulting inclusions would contain halite daughter crystals at room temperature, thus yielding information on halite solubilities where none existed previously.

The synthetic fluid inclusions appear similar to those produced in previous experiments (*e.g.*, BODNAR *et al.*, 1985). Most inclusions populate healed fracture surfaces that are planar or slightly curved. Inclusion sizes range from submicron to several tens of microns; they are usually fairly equant (Fig. 2) and distributed evenly along the healed fractures. Inclusions contain liquid, vapor, and a halite daughter crystal at room temperature. The majority have constant phase volume ratios, indicating that they contain similar bulk compositions. In addition, there exist a variable number of inclusions that are not well suited for study because it cannot be shown that they contain the desired bulk compositions. Most of these latter inclusions are large and irregular, with long thin extensions. Many appear to be filled with gas, which is probably air that entered the inclusions during the polishing. Other irregular shaped inclusions appear to have spawned nearby inclusions, often containing different phase ratios, by necking down (ROEDDER, 1984).

Sample 5, although it has a bulk composition within the halite liquidus field, contains fluid inclusions that typically do not contain halite at room temperature. Thus, the phase assemblage in these inclusions is a metastable one, a problem not uncommon in saline inclusions only slightly oversaturated with halite at room temperature (ROEDDER, 1984). By freezing and warming these inclusions through several cycles halite could be nucleated, permitting the dissolution temperatures to be determined.

In several samples (numbers 4, 6, and 9), rare birefringent phases are discernable in the large irregular shaped inclusions. Maximum interference color is first order yellow, in a grain that appears to be only about 3 microns thick. The crystals form thin blades or platelets, with maximum dimension about 3 microns. Relief and refractive indices appear to be about the same as those of halite and quartz (*i.e.*, positive relief relative to the fluid). On heating, the crystals dissolve (*e.g.*, for sample 9, birefringent crystals dissolve at around 475°C). These crystals could be quartz or wollastonite; however, the birefringence seems too high for either, and the relief seems too low for wollastonite. Regardless of the identity of the crystals none have been observed within the abundant equant inclusions that contain liquid, vapor, and halite in constant proportions; *i.e.*, in the inclusions that were taken as representative and were analyzed in this study.

### *High-temperature phase relations*

The dissolution temperature of halite daughter crystals [*Tm* (halite)] was measured to locate isotherms in the liquid + halite field. Results of 135 heating measurements from 10 samples are summarized in Table 1 and Fig. 3. The range for a given sample is generally less than 2 to 3°C (*i.e.*, nearly within the range of the maximum expected error); however, some samples exhibit substantially greater ranges. In the worst case, halite dissolution varied over a range of 11°C (12 measurements), but 10 of those twelve measurements have a range of only 3.4°C.

Nearly all inclusions underwent final homogenization *via* vapor bubble disappearance. Only in sample 3 was a subset of inclusions observed in which the vapor disappeared a few degrees before the halite. The *Tm* (halite) in both types of inclusions within sample 3, though, is indistinguishable (Table 1). For true vapor-saturated solubility determinations, the halite and the vapor bubble must disappear simultaneously.

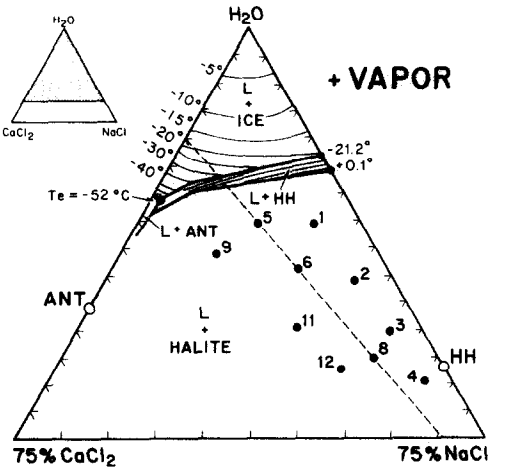


FIG. 1. Phase diagram for part of the ternary system NaCl-$CaCl_2$-$H_2O$, after YANATIEVA (1946). Compositions are in weight percent. Ternary eutectic is at about −52°C. ANT is antarcticite and HH is hydrohalite. Solid dots show bulk compositions of synthetic fluid inclusions in this study, and their sample numbers. The dashed line shows the join between $(H_2O)_{80}$-$(CaCl_2)_{20}$ and NaCl that is drawn in Fig. 5.

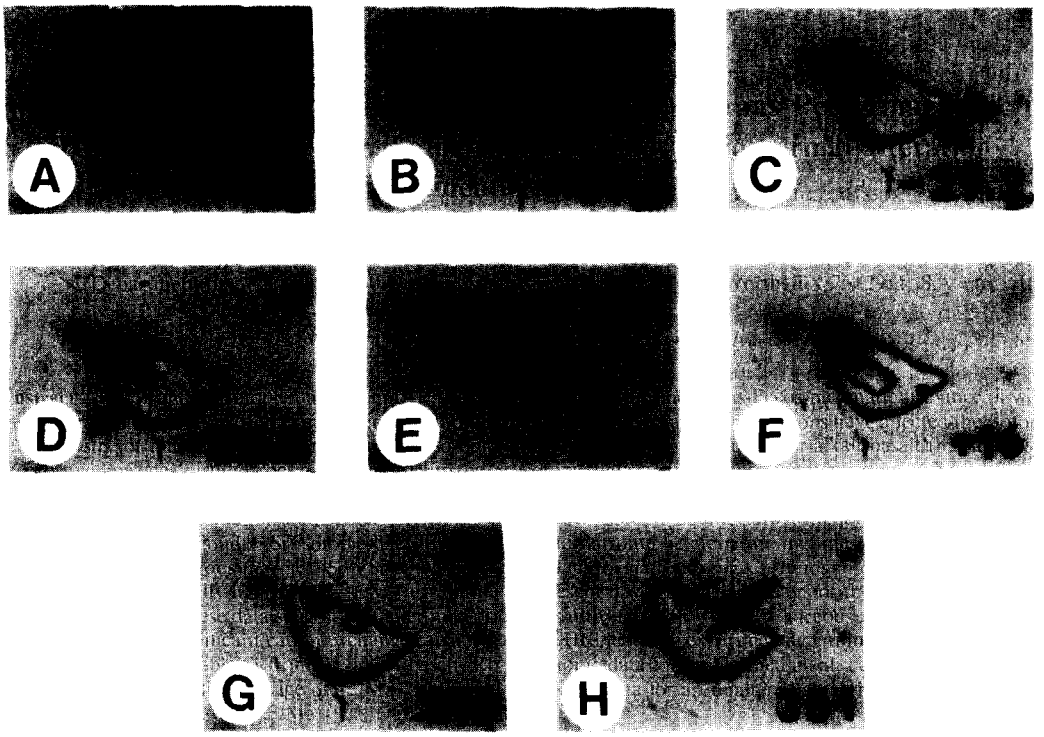


FIG. 2. Photomicrographs of sequential phase changes with varying temperature in a synthetic fluid inclusion (sample 2). The inclusion is about 33 microns long and 22 microns wide. (a) +20°C; inclusion contains liquid, vapor, and a halite daughter crystal at room temperature; (b) −41.5°C; after freezing and warming through several cycles, inclusion contains 5–6 large hydrohalite grains (low relief) and ice (moderate relief), as well as liquid (allowing the ice to appear rounded) and vapor; (c) −29.2°C; same phases as in the previous photo, but the liquid is greater and the ice (arrows) is smaller in volume; (d) −25.8°C; single tiny ice crystal (arrow) is present, and measured *Tm* (ice) is −25.5°C; (e) +1.7°C; inclusion contains liquid, vapor, and metastable hydrohalite; note that the hydrohalite is little changed from the previous photo; (f) +16.0°C; metastable hydrohalite has transformed into stable halite, but as two crystals with complex boundaries; on heating, surface energy reduction will cause the halite to recrystallize into a single crystal with simple boundaries; (g) +318°C; halite and vapor are smaller due to dissolution and volume expansion of the liquid, respectively; (h) +351°C; halite is a tiny speck (arrow), with measured *Tm* (halite) of +357°C; note that fluid at this stage approximates vapor-saturation, because vapor and halite disappearance are nearly simultaneous (see text).

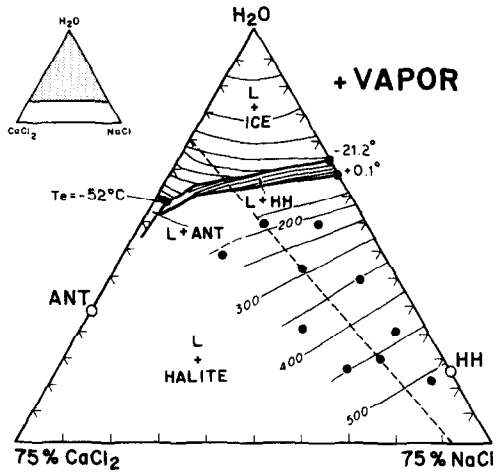


FIG. 3. Phase diagram for $NaCl-CaCl_2-H_2O$ incorporating the measured *Tm* (halite) of each of the synthetic fluid inclusions. Compositions are in weight percent. Solid isothermal contours are anchored along the $NaCl-H_2O$ binary using average halite solubilities from CHOU (1987) and STERNER *et al.* (1988). The dashed line shows the portion of the join between $(H_2O)_{80}-(CaCl_2)_{20}$ and NaCl that is drawn in Fig. 5.

In practice, it is difficult to achieve this condition. In our experiments the difference between vapor and halite disappearance was generally small, and even moderate differences have been shown to have very little effect on solubility determinations (CHOU, 1987; STERNER *et al.*, 1988).

Resulting temperature contours on the halite liquidus are nearly straight (Fig. 3), and they tie in well along the $NaCl-H_2O$ binary with data from CHOU (1987) and STERNER *et al.* (1988). The contours also parallel the trend of straight lines (hypothetical contours) that can be constructed between higher-temperature values of halite solubility along the $NaCl-H_2O$ and $NaCl-CaCl_2$ binaries (STERNER *et al.*, 1988; LEVIN *et al.*, 1969).

### *Low-temperature phase relations*

Metastable phase behavior is common in the inclusions at low temperature. For example, many of the inclusions in this study could not be frozen completely solid. This was the case particularly for the high-total salt samples (numbers 11 and 12, Fig. 1). Repeated quenching with liquid nitrogen failed to cause a change in the liquid plus vapor plus halite phase assemblage of these inclusions.

Some degree of freezing is observed in all of the other samples. By sequential freezing (HAYNES, 1985) it is easy to produce inclusions containing just a few hydrohalite and ice crystals (Fig. 2). The $CaCl_2$-rich interstitial liquid is then clearly visible and is very difficult to freeze. In fact, repeated attempts at quenching with liquid nitrogen failed to produce recognizable antarcticite, and the eutectic temperature of the system was not determined. Indirect observations of the onset of ice melting, determined by noting when euhedral ice boundaries become rounded, are often close to −52°C, but are as low as −73°C in one sample (sample 9, the most $CaCl_2$-rich one). Some of these lower temperature observations may correspond to metastable melting or recrystallization.

Relative to the fluid, ice has moderate negative relief about equal to that of halite, which has moderate positive relief (Fig. 2). Regrown ice crystals are often bladed or hexagonal tabular, the morphology depending on the available space. Ice melting [$Tm$ (ice)] was measured in the range −38.7°C to −23.3°C (Table 2).

Hydrohalite typically regrows on cooling as bladed crystals (Fig. 2). Hydrohalite melting, accompanied by growth of halite crystals with square or rectangular outlines, occurred at temperatures ranging from several degrees below zero to several degrees above zero, and is assumed to be metastable in most cases.

Observations of Becke lines indicate that ice has moderate negative relief, hydrohalite has low positive relief, and both halite and quartz have moderate positive relief relative to the fluid:

$$n_{ICE} \ll n_{FLUID} < n_{HH} < n_{HAL} \cong n_{QTZ}$$

where $n$ is average refractive index. These relations may vary depending on the fluid composition, which could explain why some previous reports differ (*e.g.*, BURRUSS and HOLLISTER, 1979, p. 167; SHEPHERD *et al.*, 1985, p. 107).

Stable phase assemblages in this system can be predicted using the phase diagram. Consider the equilibrium crystallization of a bulk composition at point a in Fig. 4 (note that the following discussion differs slightly from that of SHEPHERD *et al.*, 1985, p. 107). On cooling to the liquidus temperature (point a) halite forms and the composition of the liquid moves directly away from NaCl, assuming negligible solid solution of Ca in halite. The liquid composition reaches the halite-hydrohalite reaction curve at point b, where hydrohalite begins to form and halite begins to resorb. The liquid composition then moves down the halite-hydrohalite reaction curve toward point c. There, halite is completely resorbed (the inclusion contains hydrohalite, liquid of composition c, and vapor of negligible mass), and the liquid composition is free to move across the hydrohalite liquidus field toward point d, along a line directly away from hydrohalite. At point d ice joins the assemblage, and ice and hydrohalite co-crystallize as the liquid moves to the eutectic, point e.

Table 2. Measured Tm(ice) for synthetic inclusions

| Sample | Range | Average[1] | Predicted[2] |
|---|---|---|---|
| 1 | -23.3 to -23.9 | -23.8 (12) | -25.4 |
| 2 | -25.3 to -25.8 | -25.5 (9) | -27.4 |
| 3 | -33.7 to -37.2 | -35.5 (10) | -36.0 |
| 5 | -28.8 to -31.8 | -29.9 (3) | -33.6 |
| | -33.9 to -34.2 | -34.1 (4)[3] | |
| 6 | -37.3 to -38.7 | -38.1 (3) | -40.4 |
| | -34.1 to -34.3 | -34.2 (5)[3] | |
| 8 | -34.1 to -34.3 | -34.3 (6)[3] | |

[1] Temperatures in degrees C; number of inclusions measured in parentheses.
[2] These values determined by interpolating from Yanatieva (1946).
[3] For these inclusions, Tm(ice) is in the presence of metastable halite, not hydrohalite; see text for discussion.

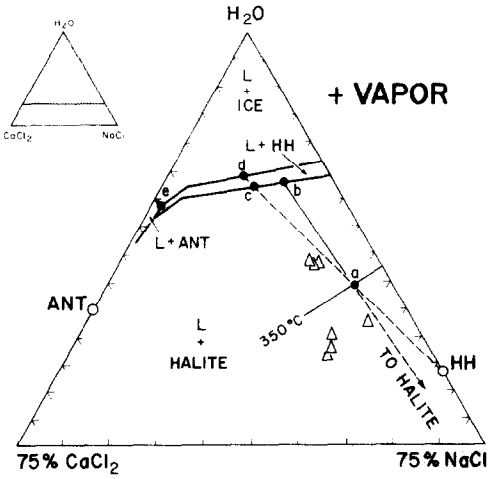


FIG. 4. Liquid line of descent for a bulk liquid composition at point a, which corresponds to sample 2 (39.6% NaCl, 6.0% $CaCl_2$, 54.4% $H_2O$). The path is discussed in the text. Triangles are the inferred natural compositions from Mathematician Ridge fluid inclusions (Table 3).

In theory the equilibrium melting path on heating is simply the reverse of the cooling path. In practice, metastability complicates both cooling and heating paths. For instance, hydrohalite persists metastably to temperatures several degrees above the expected equilibrium (ROEDDER, 1984; and see Fig. 2, for example). One equilibrium phase transition that can be reliably reproduced is the ice melting temperature (point d, Fig. 4). This has been determined for several inclusions that lose ice along the ice-hydrohalite cotectic, and results of 52 freezing measurements are given in Table 2. When compared to the temperatures predicted by extrapolation of the data of YANATIEVA (1946), differences of several tenths to less than two degrees show the consistency of the two data sets. The low angle of intersection between the isotherms and the cotectic precludes more exact agreement.

In three samples, some or all inclusions failed to nucleate hydrohalite on freezing (Table 2). In these cases, at low temperatures, the metastable ice melting temperature in the presence of halite, vapor, and liquid was determined reproducibly. In theory, this temperature should be the same for all three samples, because they all have bulk compositions along the pseudobinary between NaCl and $(CaCl_2)_{20}(H_2O)_{80}$ (Fig. 3 and Fig. 5). The actual measured temperatures differed by 0.2°C.

## APPLICATIONS TO NATURAL OCEANIC FLUID INCLUSIONS

We have used the new halite liquidus data to estimate the bulk compositions of fluid inclusions from a mid-ocean ridge

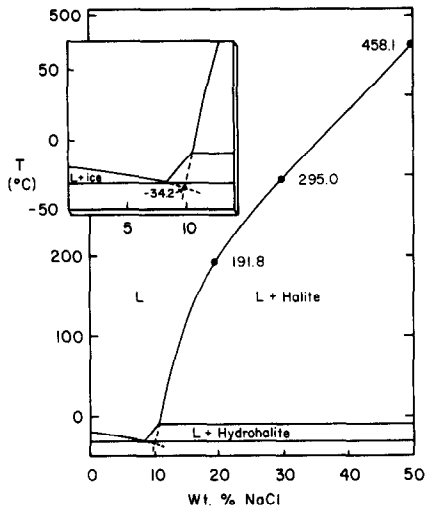


FIG. 5. Portion of the pseudobinary section of the ternary system NaCl-$CaCl_2$-$H_2O$ varying from a composition of 80 wt% $H_2O$, 20 wt% $CaCl_2$ (*i.e.*, 0% NaCl) to 100% NaCl (see Figs. 1 and 3 for location). Temperatures labelled on the liquidus have been determined in the present study, as has the temperature of ice melting in the presence of metastable halite (−34.2°C). The ice and hydrohalite liquidus curves are interpolated from data of YANATIEVA (1946).

spreading center. Quartz-veined metagabbros dredged from the Mathematician Ridge, East Pacific, contain abundant fluid inclusions (VANKO, 1988; STAKES and VANKO, 1986). Individual samples record episodes of fluid trapping ranging from as high as 700°C (primary inclusions) to 150°C (secondary inclusions). In two samples, coexisting dense halite-saturated inclusions and low-density, low-salinity vapor-rich inclusions (average 45 and 2 wt% NaCl equivalent) attest to an episode of phase separation, which is interpreted to have occurred at 600–700°C and 60–100 MPa pressure (VANKO, 1988).

Initial melting in the halite-saturated inclusions is in the range −50 to −70°C. Components such as $CaCl_2$ and $MgCl_2$ can lower the eutectic temperatures of natural NaCl-rich fluids to these values, but evidence from deep-sea hot springs strongly suggests that mature oceanic hydrothermal fluids are essentially devoid of magnesium, probably as a result of extensive cation exchange between seawater and oceanic crustal rocks within the downgoing portions of convective systems (*e.g.*, EDMOND *et al.*, 1979; MOTTL, 1983). Consequently, the inclusions are modeled in the system NaCl-$CaCl_2$-$H_2O$ (VANKO, 1988).

Reconnaissance measurements of *Tm* (ice) and *Tm* (halite) for several inclusions are shown in Table 3. Where ice melts in the presence of hydrohalite, liquid, and vapor, *Tm* (ice) is a stable equilibrium temperature analogous to point d in Fig. 4. The bulk composition of the fluid lies somewhere along the tie line between the liquid composition and the bulk composition of hydrohalite (e.g., d-c-a in Fig. 4). A second constraint on the bulk composition is obtained from *Tm* (halite). Given both *Tm* (ice) and *Tm* (halite), the bulk composition lies at the intersection of the tie line described above and the *Tm* (halite) isotherm on the halite liquidus. These two curves intersect at a relatively high angle, providing a good estimate of the bulk composition.

Several measurements of *Tm* (ice) were also made at the metastable transition when ice melts in the presence of liquid, vapor, and metastable halite. In these inclusions, halite never transformed to hydrohalite on cooling. Similar behavior was observed in several of the synthetic fluid inclusions, particularly those with high $CaCl_2$ and high total salt contents. In these cases, well-constrained bulk compositional estimates cannot be obtained because only one temperature is known along the metastable reaction curve (Fig. 5). However, assuming that the metastable curve parallels the stable ice-hydrohalite cotectic, and that temperatures along the metastable curve are uniformly about 3°C lower than the cotectic temperatures at the same $H_2O$-$CaCl_2$ ratio (*i.e.*, along pseudobinaries toward NaCl), then bulk compositions can be estimated crudely (Table 3).

The Na:Ca weight ratios determined for the natural fluid inclusions range from 2.9 to 7.3 (Table 3 and Fig. 4). These values are substantially below the seawater ratio of 26, but are close to hypothetical hydrothermal end-member fluids (*i.e.*, sampled fluids with the effects of admixed seawater removed; EDMOND *et al.*, 1979) inferred from chemical analyses of hot spring solutions. In particular, the hydrothermal end-members at the southern Juan de Fuca Ridge have Na:Ca of 4.5 to 5.8 (VON DAMM and BISCHOFF, 1987), and the 13°N East Pacific Rise end-member solution has Na:Ca of 6.1 (MICHARD *et al.*, 1984). Saline fluid inclusions from the Mathematician Ridge therefore possess Na:Ca ratios identical to those seen in some modern "black smoker" hot springs in the deep sea, although the total salinities are many times greater. Phase separation of a seawater-derived hydrothermal fluid accounts for these observations (VANKO, 1988).

## CONCLUSIONS

1. Halite solubilities in the ternary system NaCl-$CaCl_2$-$H_2O$ have been determined for compositions with as much as 25 wt% $CaCl_2$, total salinities > 60 wt%, and temperatures up to 500°C, using the synthetic fluid inclusion technique. Results appear to tie in smoothly with previous high-temperature data for the binaries NaCl-$H_2O$ and NaCl-$CaCl_2$.

2. By measuring *Tm* (ice) and *Tm* (halite) in inclusions that are saturated with halite at room temperature, the bulk compositions of inclusions can be estimated graphically.

3. Application of the technique to some natural saline inclusions from a mid-ocean ridge hydrothermal system shows that the Na:Ca ratio determined is the same as that found in active high-temperature "black smokers" on the seafloor.

Table 3. Results of heating and freezing measurements on natural fluid inclusions (temperatures in °C)

| Sample[1] | Tm(ice) | Tm(halite) | NaCl/$CaCl_2$/$H_2O$ | Na:Ca (wt) |
|---|---|---|---|---|
| B-1i | -30.9 | 278 | 30.2/10.8/59.0 | 3.0 |
| B-1k | -34.8 | 402 | 44.6/ 6.7/48.7 | 7.3 |
| A-1e | -29.9 | 288 | 31.5/10.0/58.5 | 3.4 |
| A-1c | -29.6 | 287(est) | 31.4/ 9.9/58.6 | 3.5 |
| A-1b | -30.8 | 286 | 31.0/10.5/58.5 | 3.2 |
| A-3h | -38.2[2] | 393 | 40/14/46 | 3.1 |
| A-1l | -43.5[2] | 412 | 42/16/42 | 2.9 |
| A-1n | -42.0[2] | 411 | 42/16/42 | 2.9 |

[1] All inclusions are from a quartz vein in hornblendite, sample 7-45, section II (Vanko, 1988).
[2] Metastable ice melting temperature in the presence of liquid, vapor, and metastable halite. Estimates of bulk composition are discussed in the text.

*Acknowledgements*—Synthetic fluid inclusion experiments were undertaken at Virginia Tech with the support of NSF grant EAR-8607356 to RJB and a Georgia State University Research Grant to DAV. Heating and freezing experiments of natural and synthetic inclusions were conducted at Georgia State, supported by NSF grants EAR-8316739 and OCE-8710717 to DAV. Samples from the Mathematician Ridge were graciously provided by Rodey Batiza, chief scientist for the cruise AFTERMATH. We thank Seth Rose for reading an early version of the manuscript. Reviews by F. M. Haynes, M. A. McKibben, and R. J. Spenser led to many improvements in the manuscript.

*Editorial handling:* D. M. Shaw

## REFERENCES

BODNAR R. J. and STERNER S. M. (1987) Synthetic fluid inclusions. In *Hydrothermal Experimental Techniques* (eds. G. C. ULMER and H. L. BARNES), pp. 423–457. J. Wiley & Sons, New York.

BODNAR R. J., BURNHAM C. W. and STERNER S. M. (1985) Synthetic fluid inclusions in natural quartz. III. Determination of phase equilibrium properties in the system $H_2O$-NaCl to 1000°C and 1500 bars. *Geochim. Cosmochim. Acta* **49**, 1861–1873.

BURRUSS R. C. and HOLLISTER L. S. (1979) Evidence from fluid inclusions for a paleothermal gradient at the geothermal test well sites, Los Alamos, New Mexico. *J. Volcanol. Geotherm. Res.* **5**, 163–177.

CHOU I-M. (1987) Phase relations in the system NaCl-KCl-$H_2O$. Part III: Solubilities of halite in vapor-saturated liquids above 445°C and redetermination of phase equilibrium properties in the system NaCl-$H_2O$ to 1000°C and 1500 bars. *Geochim. Cosmochim. Acta* **51**, 1965–1975.

CRAWFORD M. L. (1981) Phase equilibria in aqueous fluid inclusions. In *Short Course in Fluid Inclusions: Applications to Petrology*, (eds. L. S. HOLLISTER and M. L. CRAWFORD), pp. 75–100. Mineral. Assn. Canada.

EDMOND J. M., MEASURES C., MCDUFF R. E., CHAN L. H., COLLIER R., GRANT B., GORDON L. I. and CORLISS J. B. (1979) Ridge crest hydrothermal activity and the balances of major and minor elements in the oceans: The Galapagos data. *Earth Planet. Sci. Lett.* **46**, 1–18.

FUZIKAWA K. (1982) Fluid inclusion and oxygen isotope studies of the Nabarlek uranium deposit, N.T. Australia, Ph.D. dissertation, Univ. Adelaide.

GUNTER W. D., CHOU I-M. and GIRSPERGER S. (1983) Phase relations in the system NaCl-KCl-$H_2O$. Part II: Differential thermal analysis of the halite liquidus in the NaCl-$H_2O$ binary above 450°C. *Geochim. Cosmochim. Acta* **47**, 863–873.

HALL D. L., STERNER S. M. and BODNAR R. J. (1988) Freezing point depression of NaCl-KCl-$H_2O$ solutions. *Econ. Geol.* **83**, 197–202.

HAYNES F. M. (1985) Determination of fluid inclusion compositions by sequential freezing. *Econ. Geol.* **80**, 1436–1439.

KWAK T. A. P. and TAN T. H. (1981) The importance of $CaCl_2$ in fluid composition trends—evidence from the King Island (Dolphin) skarn deposit. *Econ. Geol.* **76**, 955–960.

LEVIN E. M., ROBBINS C. R. and MCMURDIE H. F. (1969) *Phase Diagrams for Ceramists*, 1969 Suppl. (ed. M. K. RESER). American Chemical Society, Columbus, Ohio.

LINKE W. F. (1958) *Solubilities of Inorganic and Metal-Organic Compounds*, 4th edn., 1. Van Nostrand, 1407p.

MCKIBBEN M. A., WILLIAMS A. E. and OKUBO S. (1988) Metamorphosed Plio-Pleistocene evaporites and the origins of hypersaline brines in the Salton Sea geothermal system, California: Fluid inclusion evidence. *Geochim. Cosmochim. Acta* **52**, 1047–1056.

MICHARD G. F., ALBAREDE F., MICHARD A., MINSTER J.-F., CHARLOU J.-L. and TAN N. (1984) Chemistry of solutions from the 13°N East Pacific Rise hydrothermal site. *Earth Planet. Sci. Lett.* **67**, 297–307.

MOTTL M. J. (1983) Metabasalts, axial hot springs, and the structure of hydrothermal systems at mid-ocean ridges. *Geol. Soc. Amer. Bull.* **94**, 161–180.

PAGEL M., POTY B. and SHEPPARD S. M. F. (1980) Contribution to some Saskatchewan uranium deposits mainly from fluid inclusion and isotopic data. *Proc. Intl. Uranium Symp. on the Pine Creek Geosyncline* (eds. J. FERGUSON and A. B. GOLEBY), pp. 639–654. Intl. Atomic Energy Agency.

POTTER R. W. II, BABCOCK R. S. and BROWN D. L. (1977) A new method for determining the solubility of salts in aqueous solutions at elevated temperatures. *J. Res. U.S. Geol. Surv.* **5**, 389–395.

ROBERT F. and KELLY W. C. (1987) Ore-forming fluids in Archean gold-bearing quartz veins at the Sigma Mine, Abitibi greenstone belt, Quebec, Canada. *Econ. Geol.* **82**, 1464–1482.

ROEDDER E. (1984) *Fluid Inclusions; Reviews in Mineralogy*, Vol. 12. Mineral. Soc. Amer., 644p.

SHEPHERD T., RANKIN A. H. and ALDERTON D. H. M. (1985) *A Practical Guide to Fluid Inclusion Studies*. Blackie, 239p.

SOURIRAJAN S. and KENNEDY G. C. (1962) The system $H_2O$-NaCl at elevated temperatures and pressures. *Amer. J. Sci.* **260**, 115–141.

STAKES D. S. and VANKO D. A. (1986) Multistage hydrothermal alteration of gabbroic rocks from the failed Mathematician Ridge. *Earth Planet. Sci. Lett.* **79**, 75–92.

STERNER S. M. and BODNAR R. J. (1984) Synthetic fluid inclusions in quartz: I. Compositional types synthesized and applications to experimental geochemistry. *Geochim. Cosmochim. Acta* **48**, 2659–2668.

STERNER S. M., HALL D. L. and BODNAR R. J. (1988) Synthetic fluid inclusions: V. Solubility relations in the system NaCl-KCl-$H_2O$ under vapor-saturated conditions. *Geochim. Cosmochim. Acta* **52**, 989–1005.

TAYLOR M., KESLER S. E., CLOKE P. L. and KELLY W. C. (1983) Fluid inclusion evidence for fluid mixing, Mascot-Jefferson City zinc district, Tennessee. *Econ. Geol.* **78**, 1425–1439.

VANKO D. A. (1988) Temperature, pressure, and composition of hydrothermal fluids, with their bearing on the magnitude of tectonic uplift at mid-ocean ridges, inferred from fluid inclusions in oceanic layer 3 rocks. *J. Geophys. Res.* **93**, 4595–4611.

VON DAMM K. L. and BISCHOFF J. L. (1987) Chemistry of hydrothermal solutions from the Southern Juan de Fuca ridge. *J. Geophys. Res.* **92**, 11334–11346.

YANATIEVA O. K. (1946) Polythermal solubilities in the systems $CaCl_2$-$MgCl_2$-$H_2O$ and $CaCl_2$-NaCl-$H_2O$. *Zhur. Priklad. Khim.* **19**, 709–722 (in Russian).